ENGINEERING RESEARCH JOURNAL (ERJ)
Vol. 51, No. 2 April. 2022, pp .83-101
Journal Homepage: erj.bu.edu.eg

Performance of Reinforced Engineered Cementitious Composite Beams

Osama O. El-Mahdy[a], Gehan A. Hamdy[a], Mosaad H. El-Diasity[b] and Yousry Shalaby[c]

[a]Professor of Structural Analysis, Faculty of Engineering at Shoubra, Benha University.
[b]Assistant Professor, Faculty of Engineering at Shoubra, Benha University.
[c]Teaching Assistant, Faculty of Engineering at Shoubra, Benha University.

Abstract. Engineered Cementitious Composite (ECC) was recently developed and was reported to improve the strength, damage tolerance, ductility, energy dissipation capacity, and durability of components when compared to conventional reinforced concrete. A polyvinyl alcohol fiber reinforced engineered cementitious composite (PVA-ECC) using local ingredients – namely local sand instead of using microsilica sand – was developed, aiming for tensile strain capacity matching that of steel reinforcement for commonly used reinforced concrete structures while reducing the cost. The main objectives of this research are to develop and validate a procedure for numerical modeling and structural analysis of PVA-ECC beams using local sand. Also, the research aims to study the effects of several parameters on the flexural and shear behaviors of PVA-ECC beams. The results of numerical study indicated that the PVA-ECC beams have excellent shear capacity that helps in decreasing shear reinforcement congestion in structural elements. Consequently, PVA-ECC with local sand is very useful for structural elements to resist seismic loads. Furthermore, the peak load is increased with increasing of longitudinal reinforcement ratio (μ) and with increasing of yielding stress. On the other hand, the peak load is decreased with increase of shear span-to-depth ratio (S/d) and the mid-span deflection at peak load is increased with the increasing of S/d in all cases. The stiffness of PVA-ECC is decreased with increasing of S/d and is slightly increased with increasing of μ values. Also, there are minor differences in stiffness when yielding stress of steel reinforcement is changed.

KEYWORDS: Structural Behavior, Beams, Polyvinyl Alcohol Fiber (PVA), Engineered Cementitious Composites (ECC), Numerical Modeling.

1. INTRODUCTION

Fiber-reinforced concrete is a new material that has been extensively studied and is being used increasingly by the construction industry as an alternative to normal reinforced concrete (RC). Although the use of fibers increased toughness of concrete in compression, researchers were not able to increase the ductility of concrete under tensile loading condition. However, in the 1980s and 1990s various classes of fiber reinforced composites such as Engineered Cementitious Composites (ECC) were developed for practical applications in construction. ECC exhibit a ductile response under direct tension test, this ductile behavior of ECC has made them distinct from other fiber-reinforced concrete materials. Many studies conducted on ECC indicated that use of ECC improved the strength, damage tolerance, ductility, energy dissipation capacity, and durability of components when compared to conventional reinforced concrete. Fukuyama et al. [1] carried out tension-compression reversed cyclic test and a

structural test with six beam elements. The obtained results showed that brittle failures as shear failure and bond splitting failure observed in the ordinary RC beams can be prevented by utilizing PVA-ECC instead of concrete. Therefore, it can be clarified that ECC has much feasibility to amend the structural behavior and damage tolerance of structural elements. Li and Wang [2] tested three series of ECC beams reinforced using GFRP with various shear span-to-depth and longitudinal reinforcement ratios. The results showed that, under the same reinforcement configurations, ECC beams exhibit significant improvement in flexural behavior in terms of ductility, load-carrying capacity, shear resistance, and damage tolerance compared with the counterpart high-strength concrete (HSC) beam. Hemmati et al. [3] carried out experimental and parametric studies to evaluate the influence of using High Performance Fiber Reinforced Cementitious Composite (HPFRCC). The analytical and experimental results showed that, using HPFRCC material instead of normal concrete in RC beams increased the ultimate load, deflection, ductility ratio, plastic hinge length and rotation capacity compared to RC beams. Yuan et al. [4] tested ECC or ECC/concrete composite beams reinforced using basalt fiber-reinforced polymer (BFRP). The experimental results showed that, BFRP-reinforced ECC beams had much better flexural properties in terms of load-carrying capacity, shear resistance, ductility, and damage tolerance compared with BFRP-reinforced concrete beams. Qudah and Maalej [5] evaluated the possibility of using ultra-ductile Engineered Cementitous Composites (ECC) to improve the behavior of beam–column connections. The obtained test results showed that, the use of ECC material in the connection plastic zone as a replacement of concrete and partial replacement of transverse reinforcement can significantly improve the joint shear resistance, energy absorption capacity, and cracking response. Alyousif et al. [6] conducted experimental works to investigate the shear behavior of reinforced ECC and normal concrete (NC) beams with different shear span ratios. The test results indicated that the behavior of ECC beams under shear was much better than that of NC beams. Moreover, the strength, stiffness, ductility and energy absorption capacity of the ECC beams were found to be significantly higher than those of the corresponding NC beams. Said et al. [7] investigated the flexural performance of ECC concrete beams reinforced with innovative hybrid bars. Twelve half-scale ECC-concrete beams were tested to study the flexure behavior under four-points loading test using PVA-ECC fibers. The experimental variables were the hybrid reinforcement ratios, PVA fiber ratio and hybrid and GFRP bars. The test results showed significant enhancement in the capacity of ECC concrete beams reinforced with hybrid bars or hybrid schemes. The achieved enhancements are 12% and 27% for PVA ratio of 0.75% and 1.5%, respectively. In the presence of PVA fibers, the ultimate strain of the bars is higher than that registered in the absence of PVA fibers. Meng et al. [8] developed PVA-ECC using local ingredients-namely local sand instead of using microsilica sand. Their objective was to reduce cost and tensile strain capacity. When tensile strain capacity of PVA-ECC beyond 1%, compatibility between tensile strain of PVA-ECC and tensile strain of steel is occurred. Thus, an ECC matrix with a slightly lower tensile strain by using local sand required for optimal design and to take full advantage of the ECC material. The authors achieved a theoretical relationship on the tensile strength between specimens with 2D and 3D fiber distribution. Feng et al. [9] developed ECC with Chinese local ingredients aiming to reduce the cost and match a tensile strain capacity of 4%. Compression, tension and bending tests were carried out to determine the mechanical performance of this composite material. In addition, a numerical study to characterize the tensile and flexural behaviors of ECC specimens was conducted. The effect of fiber reinforcement was investigated. Results indicated that the validated ECC numerical model realistically predicts the tension response of dogbone specimens. In addition, typical multi-cracking phenomenon and strain-hardening behavior of ECC were successfully captured. Finally, the effect of fiber length on ECC tensile response was further studied, and the results suggested that the best tensile performance of ECC is obtained for 18-mm-long PVA fiber reinforcement.

The main objectives of this research are to develop and validate a procedure for numerical modeling and structural analysis of PVA-ECC beams using local sand then study different parameters such as shear span-to-depth ratio, shear reinforcement ratio, longitudinal reinforcement ratio and yielding stress

of reinforcement on the flexural and shear behaviors of PVA-ECC beams. The developed procedure is then utilized to understand the behavior of PVA-ECC beams in both flexural and shear failures.

2. CONSTITUTIVE MODELING OF ECC MATERIALS

2.1 Behavior of ECC in Compression

Yuan et al. [4] proposed a trilinear simulation model shown in Fig.1 to predict the behavior of ECC in compression with the assumption that plane sections remain plane throughout deformation. The constitutive stress-strain relationship for compressive stress σ_c can be expressed as follows:

$$z\sigma_c = \begin{cases} 2\frac{\sigma_{co}}{\varepsilon_{co}}\varepsilon & 0 \ll \varepsilon < \frac{1}{3}\varepsilon_{co} \\ \frac{2}{3}\sigma_{co} + \frac{\sigma_{co}}{2\varepsilon_{co}}\left(\varepsilon - \frac{\varepsilon_{co}}{3}\right) & \frac{1}{3}\varepsilon_{co} \le \varepsilon < \varepsilon_{co} \\ \sigma_{co} + (\sigma_{cu} - \sigma_{co})\left(\frac{\varepsilon - \varepsilon_{co}}{\varepsilon_{cu} - \varepsilon_{co}}\right) & \varepsilon_{co} \le \varepsilon < \varepsilon_{cu} \end{cases} \quad (1)$$

Where σ_{co}= compressive strength; ε_{co}= strain at peak stress; σ_{cu}= ultimate compressive stress and ε_{cu}= ultimate compressive strain. In the current work, it is assumed that σ_{cu}= 0.50 σ_{co} and ε_{cu}= 1.50 ε_{co}.

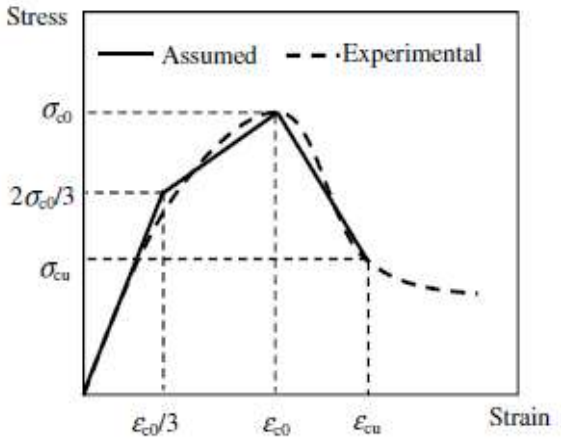

Fig. 1. Stress-strain relationship of ECC in compression [4]

2.2 Behavior of ECC in Tension

For an ECC member under uniaxial tension, after first cracking, tensile load capacity continues to increase. The strain hardening behavior is accompanied by the formation of multiple cracks. The bilinear simulation model shown in Fig. 2 was proposed by Yuan et al. [4] to predict the behavior of ECC in tension. The constitutive stress-strain relationship for tensile stress σ_{ct} can be expressed as follows:

$$\sigma_{ct} = \begin{cases} \frac{\sigma_{tc}}{\varepsilon_{tc}}\varepsilon & 0 \ll \varepsilon < \varepsilon_{tc} \\ \sigma_{tc} + (\sigma_{tu} - \sigma_{tc})\left(\frac{\varepsilon - \varepsilon_{tc}}{\varepsilon_{tu} - \varepsilon_{tc}}\right) & \varepsilon_{tc} \le \varepsilon < \varepsilon_{tu} \end{cases} \quad (2)$$

Where σ_{tc}= first cracking tensile strength; ε_{tc}= strain at first cracking; σ_{tu}= ultimate tensile strength and ε_{tu}= ultimate tensile strain.

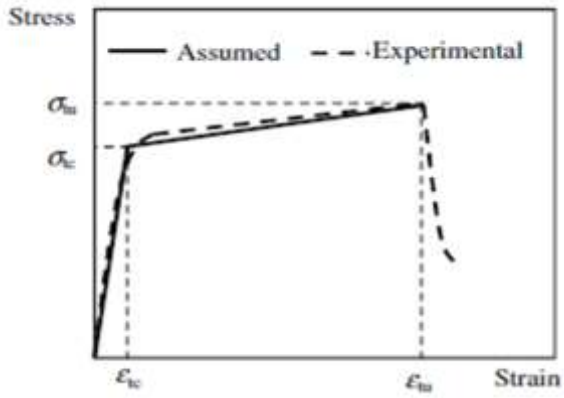

Fig. 2: Stress-strain relationship of ECC in tension [4]

2.3 Constitutive Models of ECC in ABAQUS Computer Program

ECC is modeled as concrete damage plasticity model (CDPM) presented by Lubliner et al [10] and Yu et al. [11] which is a continuum plasticity-based damage model. By adopting the concept of anisotropic damage in combination with isotropic tensile and compressive plasticity, the model can provide types of loading paths [12] and [13]. The most important parameter in CDPM is damage evolution. Generally, in order to consider the nonlinearity and irreversible deformation of concrete, the total strain ε can be consisted of two parts according to the classical elasto-plasticity theory as follows:

$$\varepsilon = \varepsilon^{el} + \varepsilon^{pl} \quad (3)$$

Where ε^{el} and ε^{pl} are the elastic and plastic strains,

respectively. Several experimental researches concluded that the nonlinearity of concrete can be contributed to the damage, plasticity or both. Whereas, the degradation of unloading stiffness is mainly associated with the damage evolution. Consequently, during the numerical modeling, it is better to sperate the effect of damage from that of plasticity.

A general ability for modeling progressive material damage can be obtained in CDPM, by introducing a scalar damage variable "*d*" that ranging between zero and one. In the case of uniaxial monotonic loading conditions, uniaxial compressive and tensile damages d_c and d_t, can be obtained by the following Equations:

$$\sigma_c = (1 - d_c)\, E_o\left(\varepsilon_c - \varepsilon_c^{pl}\right) \quad (4)$$

$$\sigma_c = (1 - d_t)\, E_o\left(\varepsilon_t - \varepsilon_t^{pl}\right) \quad (5)$$

where E_o is the initial elastic modules of concrete.
The stress-strain relationships of CDPM in compression and tension states that available in ABAQUS program are shown in Fig. 3.

Due to the lack of a complete understanding about concrete failure mechanism, a conclusive relationship between the stress state and material degradation quantitatively has not been achieved. Thus, for simplicity, the variable *d* is just defined as a linear function of stress at the softening region as follows:

$$d = 1 - \frac{\sigma^*}{\sigma_0} \quad (6)$$

Eight-node brick element (C3D8R) was used for modeling ECC. C3D8R is a general-purpose linear brick element, with reduced integration (one integration point). Two-node 3D truss element (T3D2) was used for modeling steel rebar and stirrups.

To investigate the influence of the finite element mesh refinement on the cracking behavior of the ECC and its ultimate load carrying capacity, a sensitivity analysis is performed using three different element sizes. C3D8R elements with dimensions 25, 50 and 75 mm (M25 – M50 and M75) are used for each case study.

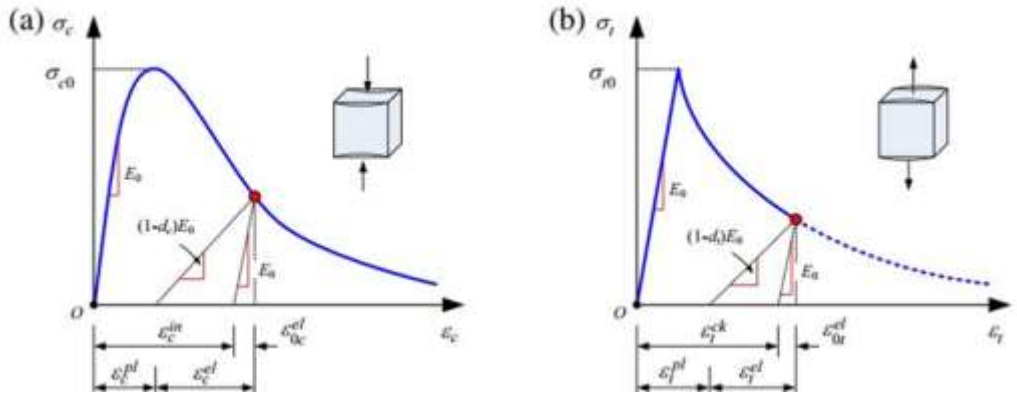

Fig. 3 Compressive and tensile stress-strain relationships of CDPM in ABAQUS

3. VALIDATION STUDY

The developed numerical model was validated against experimental results. After that, studying the effect of various parameters via this modeling approach was conducted. Therefore, the need for time consuming and costly experimental testing can be minimized. The finite element models for verification purpose were created by the nonlinear finite element analysis program ABAQUS 6.14 [14].

3.1 Verification Case Study No.1

Bastian et al. [15] presented experimental and numerical studies to investigate the flexural behavior of reinforced PVA-ECC beams. The beams had length of 2000 mm and a rectangular cross section of 100 mm x 200 mm, as shown in Fig. 4. The PVA-ECC beams were designed to be under-reinforced with three 10 mm diameter bars in the tension zone and two 10 mm diameter bars in the compression zone. Stirrups with 8 mm diameter were used throughout the shear span at a center-to-center spacing of 100 mm. The compressive strength was 46.2 MPa. The average initial cracking strength and corresponding strain were 3 MPa and 0.00013, respectively. The ultimate tensile strength and corresponding strain were 5 MPa and 0.045, respectively. The ultimate tensile strength and ultimate tensile strain are defined as the peak strength and corresponding strain. The mix proportion of ECC and PVA properties are shown in Tables 1 and 2.

Finite element models were made for the beam utilizing three mesh sizes M25, M50 and M75, and nonlinear analysis was conducted until failure. The load deflection curves obtained from the three finite element models compared with the experimental results as well as numerical results obtained by Bastian et al. [15] are shown in Fig. 5. The model with mesh size 25 mm captures the experimental test result and numerical results are better than the other numerical models. From the experimental test the average peak load and the corresponding mid-span deflection of the ECC beams are 80.39 kN and 48.94 mm, respectively. From M25 model in this work, the peak load and the corresponding mid-span deflection are 80.50 kN and 49.51 mm, respectively. From the experimental test the average yielding load and the corresponding mid-span deflection of the ECC beams are 78.22 kN and 12.01 mm, respectively with stiffness 3.72 kN/mm. From finite element analysis model in this work, the yielding load and the corresponding mid-span deflection are 76.50 kN and 9.36 mm, respectively with stiffness 8.49 kN/mm. The experimental and this work initial cracking appeared in the flexural span at an average load of 20.3 kN and 19 kN, respectively. Figure 6 shows the experimental and numerical mode of failure. It can be noted that, the failure mode obtained from experimental and finite element modeling are identical.

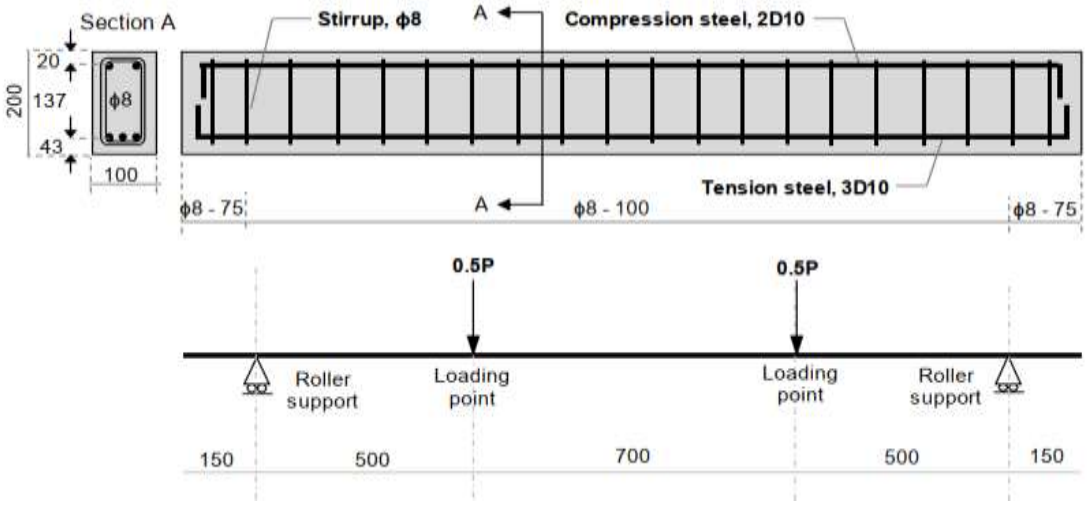

Fig. 4. Longitudinal and cross section of the beams [15]

Table 1. Mix proportion of ECC

CEM I	Silica Sand	Flay Ash	Water	HRWR	PVA	Water -to - Binder
Kg/m^3						
465	390	744	338	3.25	26	0.28

Table 2. Properties of PVA fiber

Fiber Diameter (µm)	Length (mm)	Specific Gravity (g/cm^3)	Tensile strength (MPa)	Elongation (%)	Young 's Modulus (GPa)
40	8	1.3	1600	6	41

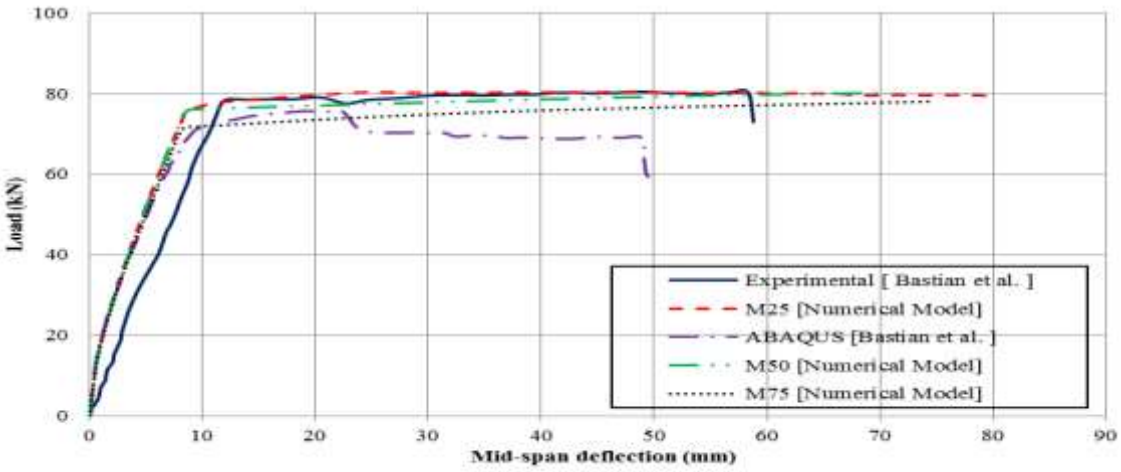

Fig. 5. Experimental and numerical mid-span load deflection relationships

i) Experimental [15]

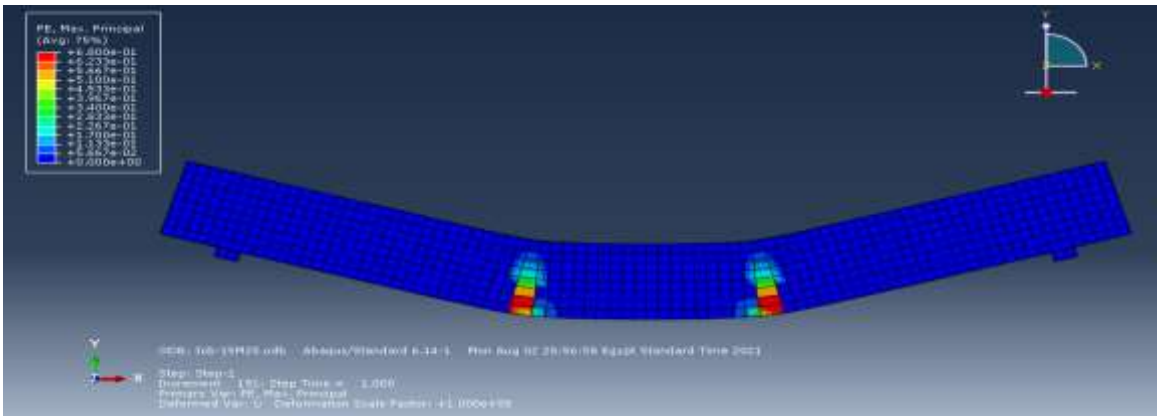

ii) Numerical model

Fig. 6. Experimental and numerical failure modes

3.2 Verification Case Study No. 2

Fang et al. [16] studied the flexural behaviors of the steel reinforced ECC and ECC/concrete composite beams using the finite element software ATENA and compared the numerical results with the experimental results of the specimens with the same geometric and mechanical properties. The beam had length of 2350 mm and a rectangular cross section of 300 mm x 200 mm as shown in Fig. 7. The ECC beam was reinforced with two 20mm diameter bars for tensile longitudinal reinforcement and two 8mm diameter bars for compressive longitudinal reinforcement. The beam was designed with dense stirrups with diameter 8 mm and spacing of 100 mm in the shear span to avoid brittle shear failure. The compressive strength and corresponding strain are 38.3 MPa and 0.004, respectively, the Young's modulus is 19.15 GPa. The average initial cracking strength and corresponding strain are 3 MPa and 0.00021, respectively. The ultimate tensile strength and corresponding strain are 4.5 MPa and 0.03, respectively. The ultimate tensile strength and ultimate tensile strain are defined as the peak strength and corresponding strain. For the mechanical properties of steel reinforcement, the 20 mm diameter steel bar has 470 MPa yield strength, 615 MPa ultimate strength, 0.08 ultimate strain and 204 GPa modulus of elasticity, while the 8 mm diameter steel bar has 460 MPa yield strength, 600 MPa ultimate strength, 0.08 ultimate strain and 200 GPa modulus of elasticity.

The load deflection curve of finite element models with the three mesh sizes M25, M50 and M75 compared with the experimental results as well as numerical results using ATENA software are shown in Fig. 8.

The model with mesh size 25 mm captures the experimental test result and yields better numerical results than the other numerical models. From the experimental test, the average peak load and the corresponding mid-span deflection of the ECC beams are 200.40 kN and 13.25 mm, respectively. From ATENA numerical simulation the peak load and the corresponding mid-span deflection are 228.36 kN and 9.72 mm, respectively. From M25 model in this work, the peak load and the corresponding mid-span deflection are 219.0 kN and 13.01 mm, respectively. From the experimental test the average yielding load and the corresponding mid-span deflection of the ECC beams are 182.53 kN and 8.52 mm, respectively with stiffness 21.42 kN/mm. From ATENA numerical simulation the yielding load and the corresponding mid-span deflection are 220.3 KN and 7.38 mm, respectively with stiffness 29.85. From finite element analysis models in this work, the yielding load and the corresponding mid-span deflection are 204.9 kN and 7.72 mm respectively with stiffness 26.54 kN/mm. Figure 9 shows the mode of failure obtained from present numerical model.

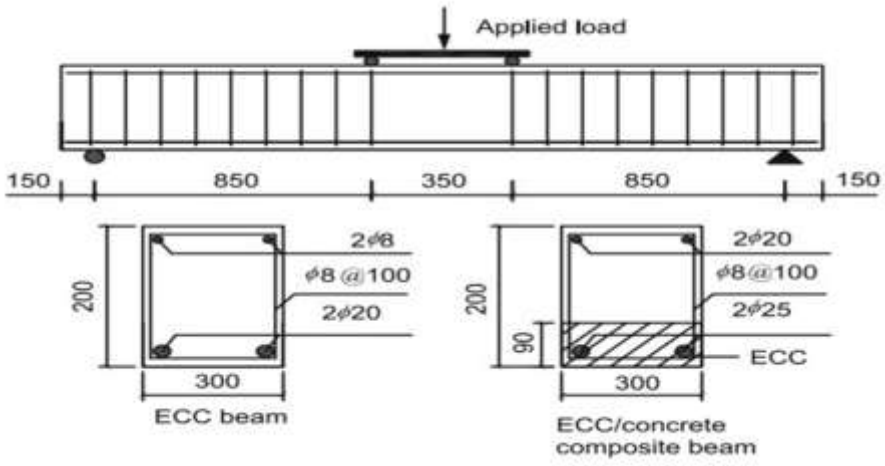

Fig.7. Longitudinal and cross section of the beams studied by Fang et al. [16]

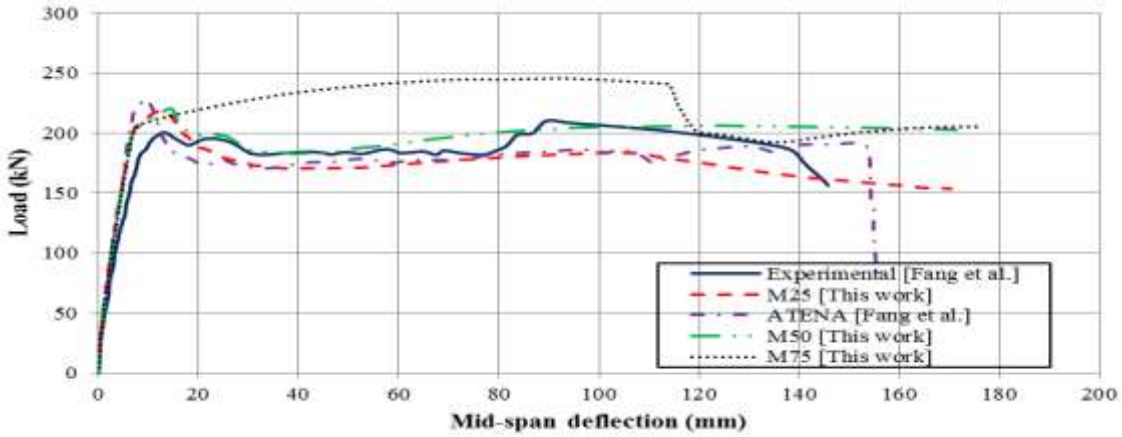

Fig. 8. Experimental and numerical mid-span load deflection relationships

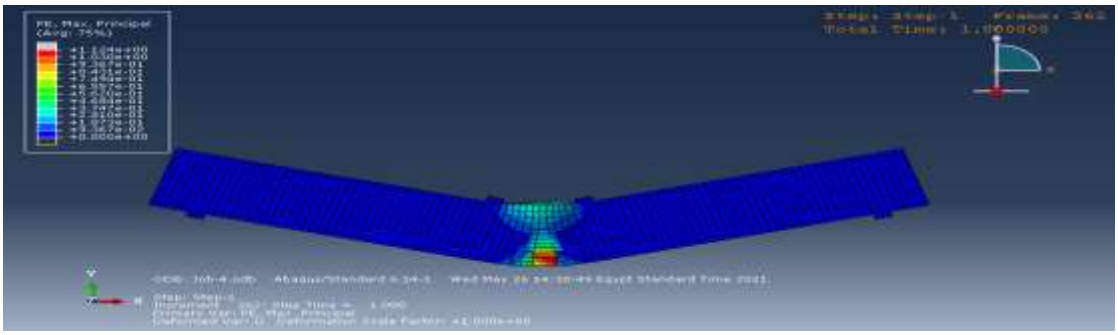

Fig. 9: Numerical failure mode

4. PARAMETRIC STUDY

Parametric study is conducted to investigate the effect of different parameters, such as shear span-to-depth ratio (S/d), shear reinforcement ratio, longitudinal reinforcement ratio (μ) and yielding stress of reinforcement (Fy) on the flexural and shear behavior of PVA-ECC beams. All the PVA-ECC beams have the ingredients, cross-sectional dimensions of the specimens tested by Meng et al. [17]. Table 3 shows the mix proportion of used PVA-ECC in all beams for parametric study. The PVA fibers had a length of 12 mm, a diameter of 39 μm and nominal strength of 1620 MPa. Figure 10 shows the schematic diagram for the studied beam and Table 4 summarizes the different parameters used in this study.

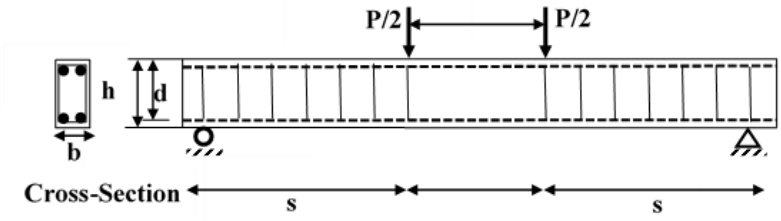

Fig. 10: Schematic diagram for the beams

Table 3. Mix proportion of ECC

Cement	Fly ash	Sand/binder	Water/binder	HRWR	Fiber (Vol.%)
1	1.2	0.36	0.3	0.01	2.2

Table 4. Summary of parametric study

Name	Matrix Properties				Cross Section			Shear Span – To - Depth Ratio (S/d)	Transverse RFT			Longitudinal Bottom RFT				
	Type	fc'	f_t	f_{tp}	b	h	d		d	Area	Spacing	Type	d	Area	μ	Fy
		MPa			mm				mm	mm^2	mm		mm	mm^2		MPa
B 01	ECC-PVA	47.1	4.1	4.8	100	200	180	1.00	—	—	—	Steel	10	157	0.87%	350
B 02									6	28.30	100					
B 03									8	50.30						
B 04								2.00	—	—	—					
B 05									6	28.30	100					
B 06									8	50.30						
B 07								3.33	—	—	—					
B 08									6	28.30	100					
B 09									8	50.30						
B 10								5.00	—	—	—					
B 11									6	28.30	100					
B 12									8	50.30						
B 13	ECC-PVA	47.1	4.1	4.8	100	200	180	1.00	—	—	—	Steel	12	226	1.25%	350
B 14									6	28.30	100					
B 15									8	50.30						
B 16								2.00	—	—	—					
B 17									6	28.30	100					
B 18									8	50.30						
B 19								3.33	—	—	—					
B 20									6	28.30	100					
B 21									8	50.30						
B 22								5.00	—	—	—					
B 23									6	28.30	100					
B 24									8	50.30						

Table 4 (cont.). Summary of parametric study

Name	Matrix Properties				Cross Section			Shear Span – To - Depth Ratio (S/d)	Transverse RFT			Longitudinal Bottom RFT				
	Type	fc'	f_t	f_{tp}	b	h	d		d	Area	Spacing	Type	d	Area	μ	F_y
		MPa			mm				mm	mm^2	mm		mm	mm^2		MPa
B 25	ECC-PVA	47.1	4.1	4.8	100	200	180	1.00	—	—	—	Steel	16	402	2.23%	350
B 26									6	28.30	100					
B 27									8	50.30						
B 28								2.00	—	—	—					
B 29									6	28.30	100					
B 30									8	50.30						
B 31								3.33	—	—	—					
B 32									6	28.30	100					
B 33									8	50.30						
B 34								5.00	—	—	—					
B 35									6	28.30	100					
B 36									8	50.30						
B 37	ECC-PVA	47.1	4.1	4.8	100	200	180	1.00	—	—	—	Steel	10	157	0.87%	420
B 38									10	78.50	100					
B 39											50					
B 40								2.00	—	—	—					
B 41									10	78.50	100					
B 42											50					
B 43								3.33	—	—	—					
B 44									10	78.50	100					
B 45											50					
B 46								5.00	—	—	—					
B 47									10	78.50	100					
B 48											50					

Table 4 (cont.). Summary of parametric study

Name	Matrix Properties				Cross Section			Shear Span – To - Depth Ratio (S/d)	Transverse RFT			Longitudinal Bottom RFT				
	Type	fc'	f_t	f_{tp}	b	h	d		d	Area	Spacing	Type	d	Area	μ	F_y
		MPa			mm				mm	mm^2	mm		mm	mm^2		MPa
B 49	ECC-PVA	47.1	4.1	4.8	100	200	180	1.00	—	—	—	Steel	12	226	1.25%	420
B 50									10	78.50	100					
B 51											50					
B 52								2.00	—	—	—					
B 53									10	78.50	100					
B 54											50					
B 55								3.33	—	—	—					
B 56									10	78.50	100					
B 57											50					
B 58								5.00	—	—	—					
B 59									10	78.50	100					
B 60											50					
B 61	ECC-PVA	47.1	4.1	4.8	100	200	180	1.00	—	—	—	Steel	16	402	2.23%	420
B 62									10	78.50	100					
B 63											50					
B 64								2.00	—	—	—					
B 65									10	78.50	100					
B 66											50					
B 67								3.33	—	—	—					
B 68									10	78.50	100					
B 69											50					
B 70								5.00	—	—	—					
B 71									10	78.50	100					
B 72											50					

4.1 Effect of Shear Reinforcement

From the load-deflection curves shown in Figs. 11 and 12, it can be noted that approximately there is no differences in behavior, stiffness and peak load points when shear reinforcement changed. This observation is valid for all shear span–to–depth (S/d) and different longitudinal reinforcement (μ) ratios. On the other hand, for beams (B39, B51, B63) with S/d = 1 the peak load is increased when using 10 mm diameter stirrups with 50 mm spacing than other beams with different shear reinforcement.

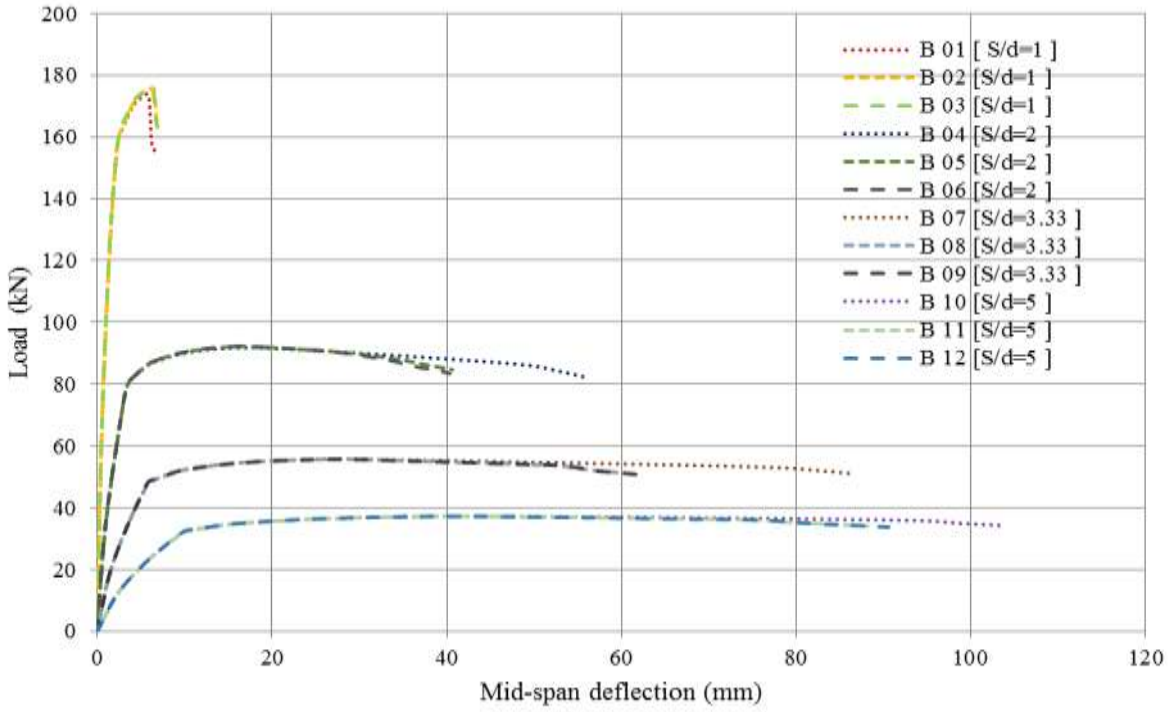

a) μ = 0.87%

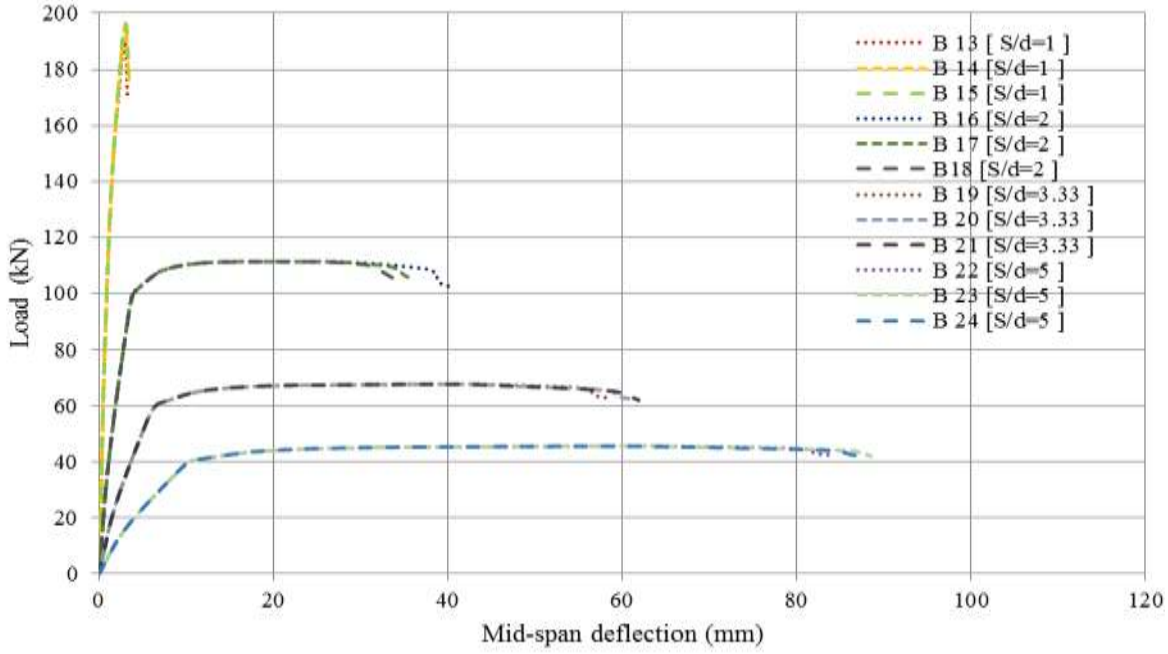

b) μ = 1.25%

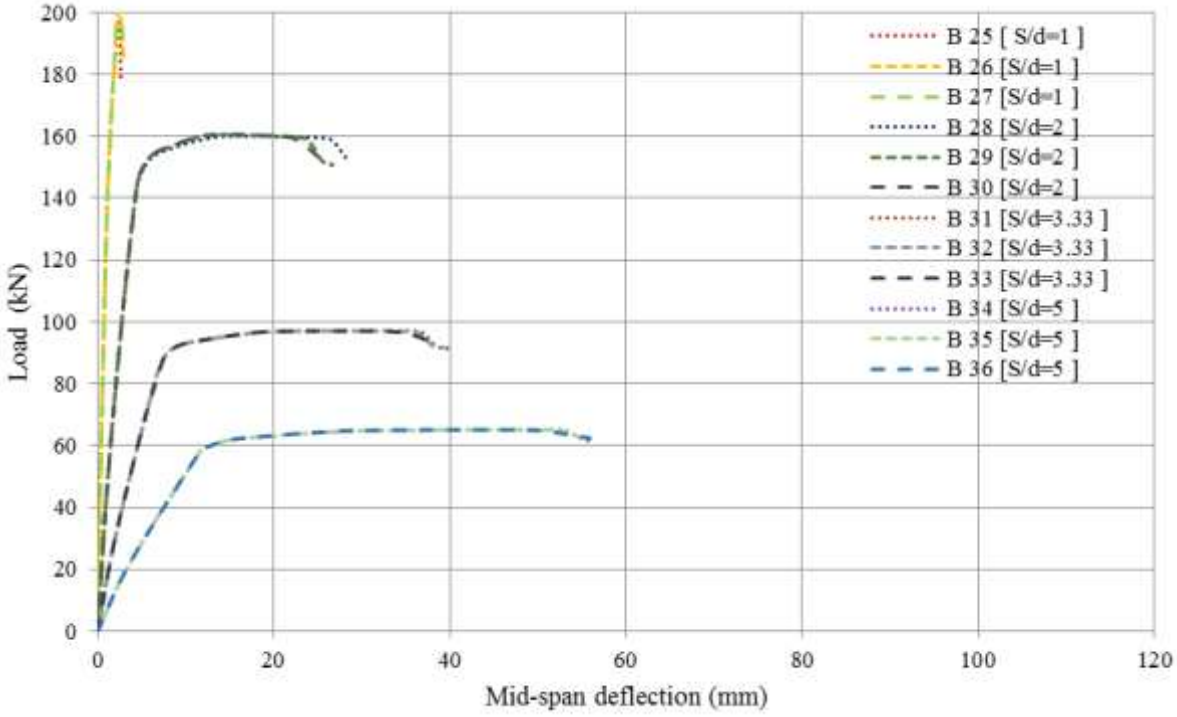

c) $\mu = 2.23\%$

Fig. 11. Load – deflection curves for beams B01 to B36

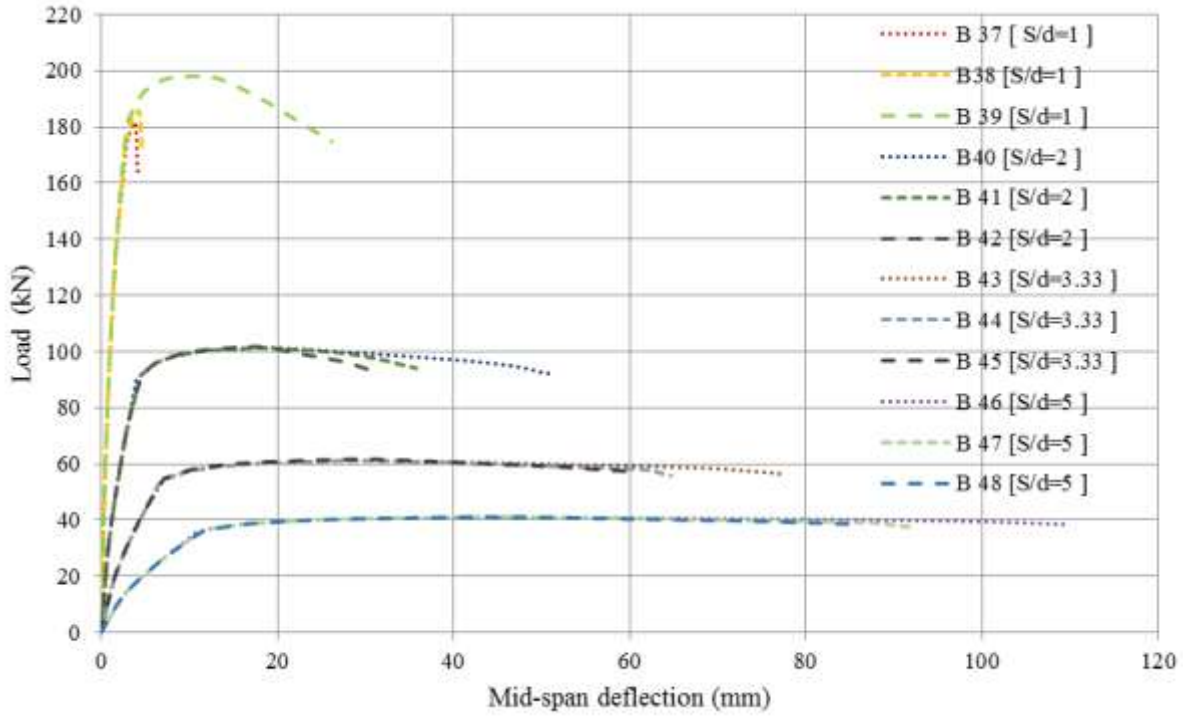

a) $\mu = 0.87\%$

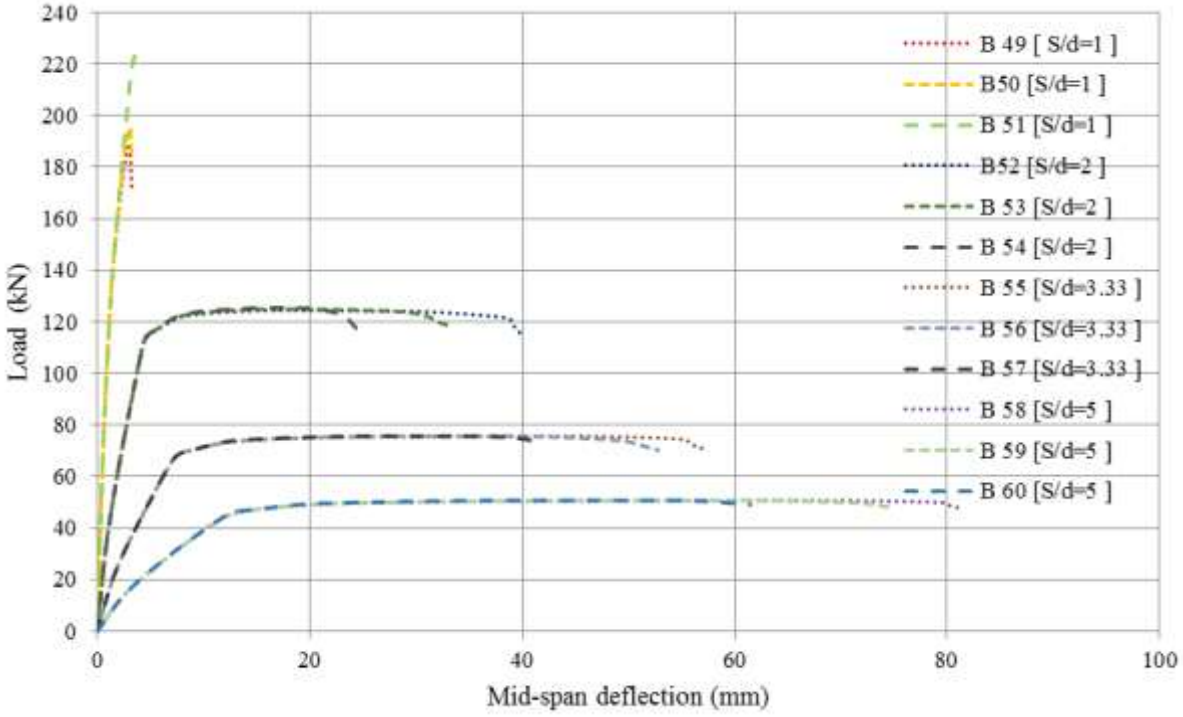

b) μ = 1.25%

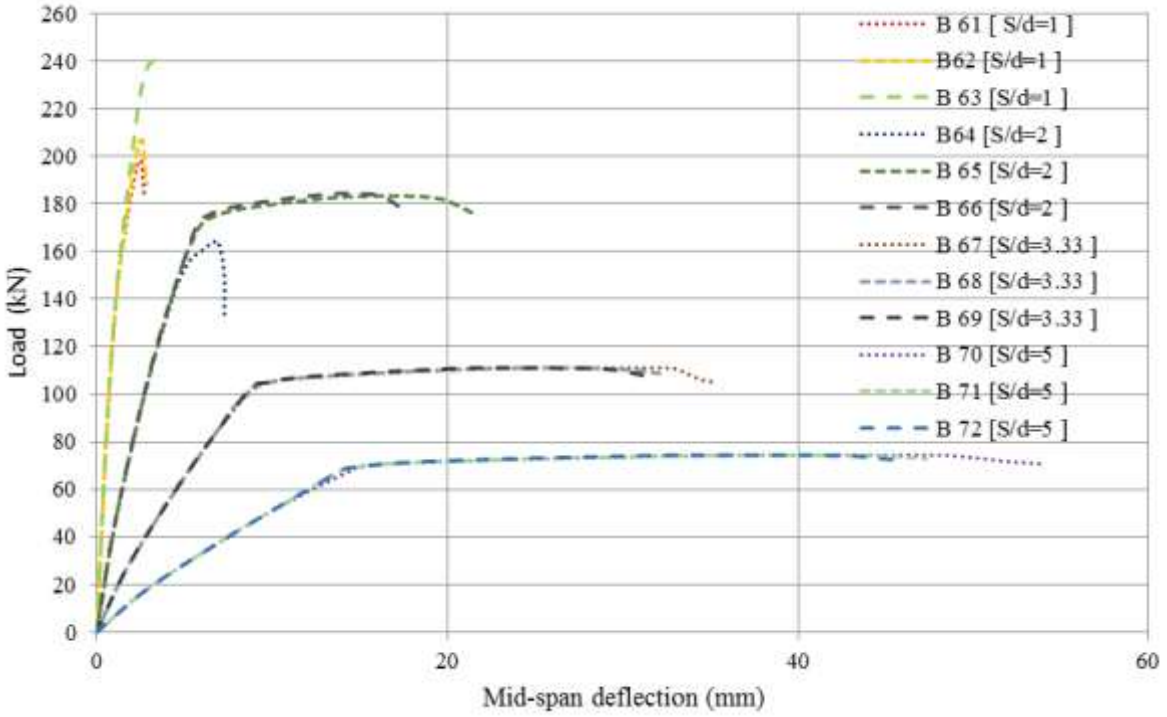

c) μ = 2.23%

Fig. 12. Load – deflection curves for beams B37 to B72

4.2 Effect of Shear Span–to–Depth and Longitudinal Reinforcement Ratios.

In general beams with S/d = 1 present a shear failure for different longitudinal reinforcement ratios. Beams with S/d ratios equal to 2, 3.33 and 5 present pure flexural failure for different longitudinal reinforcement ratios as shown in Fig. 13.

It can be noted that, the peak load decreases with the increase of S/d and increases with the increase of μ. The mid-span deflection corresponding to peak load is increased with the increase of S/d but beams with μ = 1.25% have higher values of mid-span deflection than beams with μ equal to 0.87% and 2.23% for different values of μ as shown in Fig. 14.

When S/d ratio changes from 1 to 5 the stiffness is decreased, on the other hand the stiffness is increased with the increase of μ as shown in Fig. 15. The ductility is decreased with the increase of μ as shown in Fig. 16.

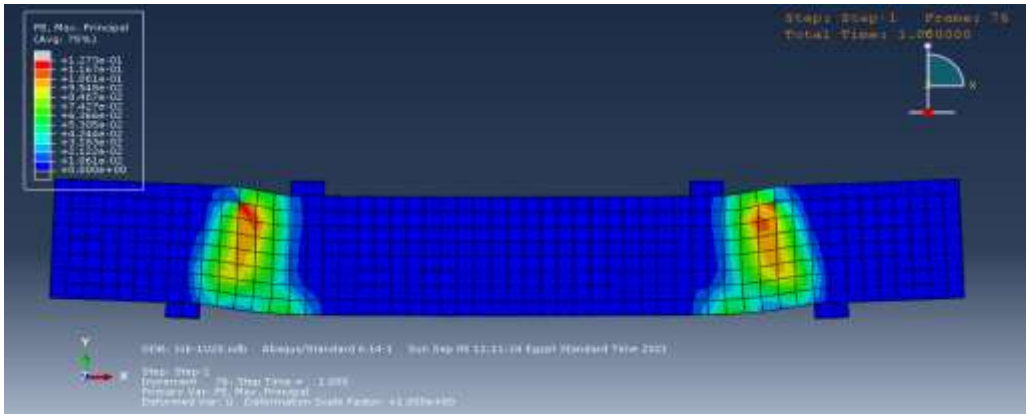

a) S/d= 1

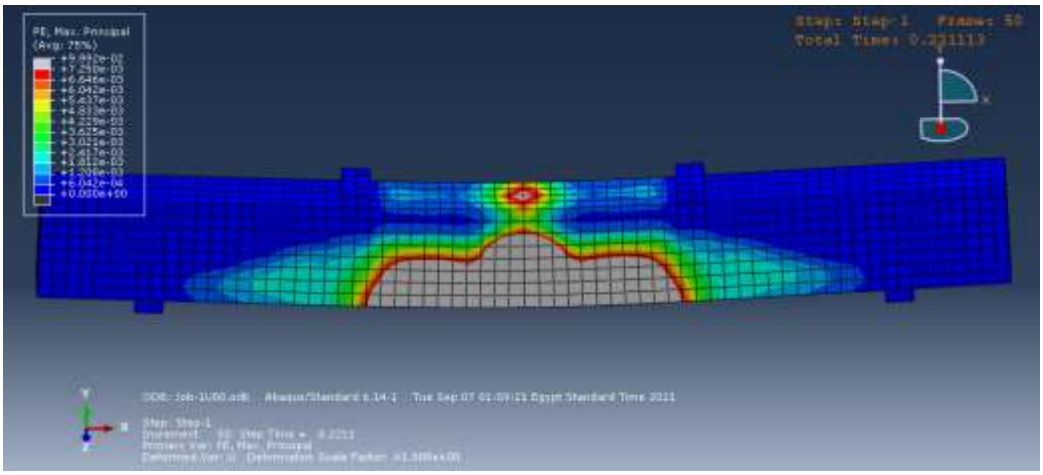

b) S/d= 2

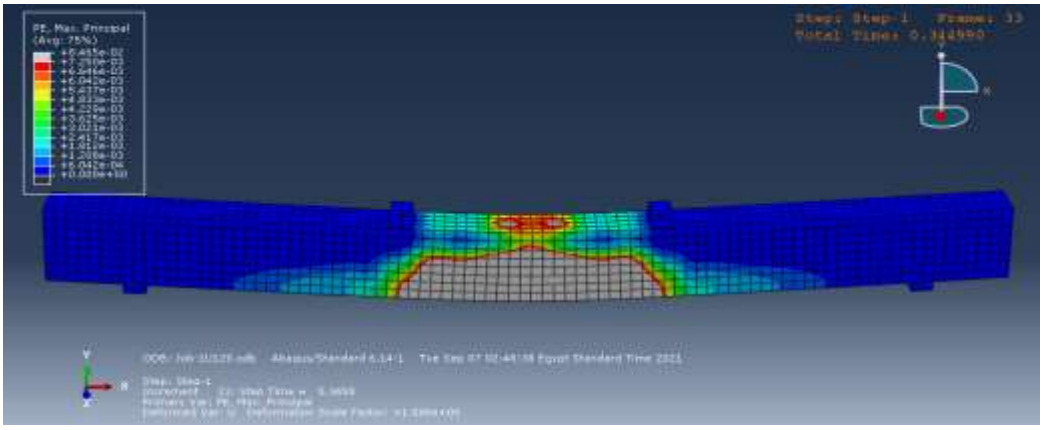

c) S/d= 3.33

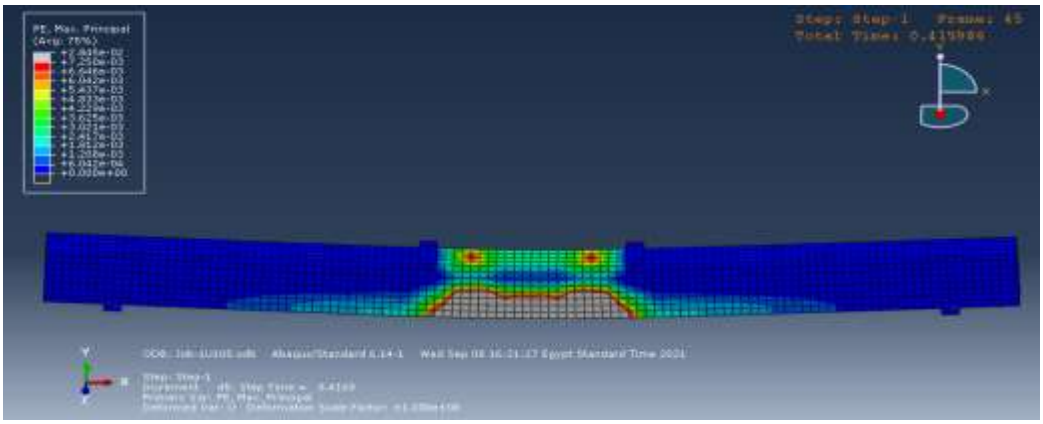

d) S/d= 5

Fig. 13. Effect of S/d on failure mode

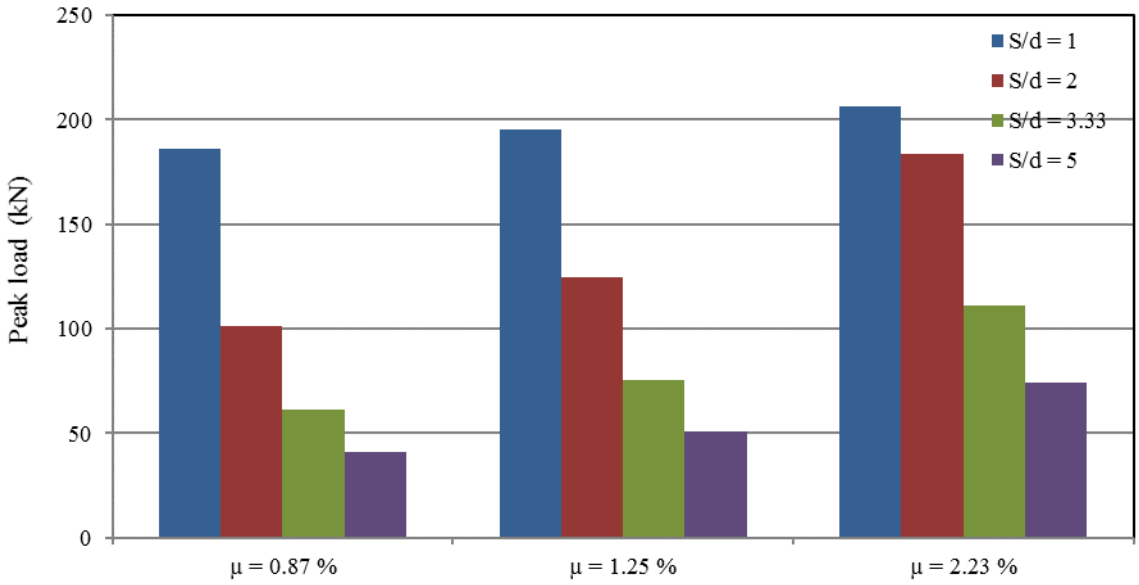

a) Effect of S/d and μ on peak load

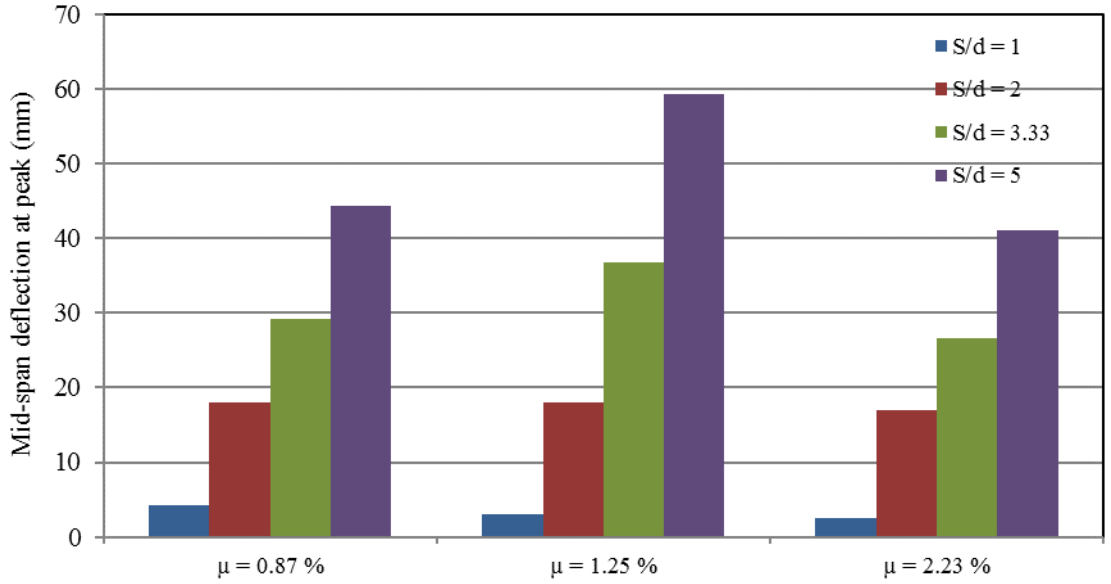

b) Effect of S/d and μ on mid-span deflection at peak load

Fig. 14. Effect of S/d and μ on peak load and mid-span deflection

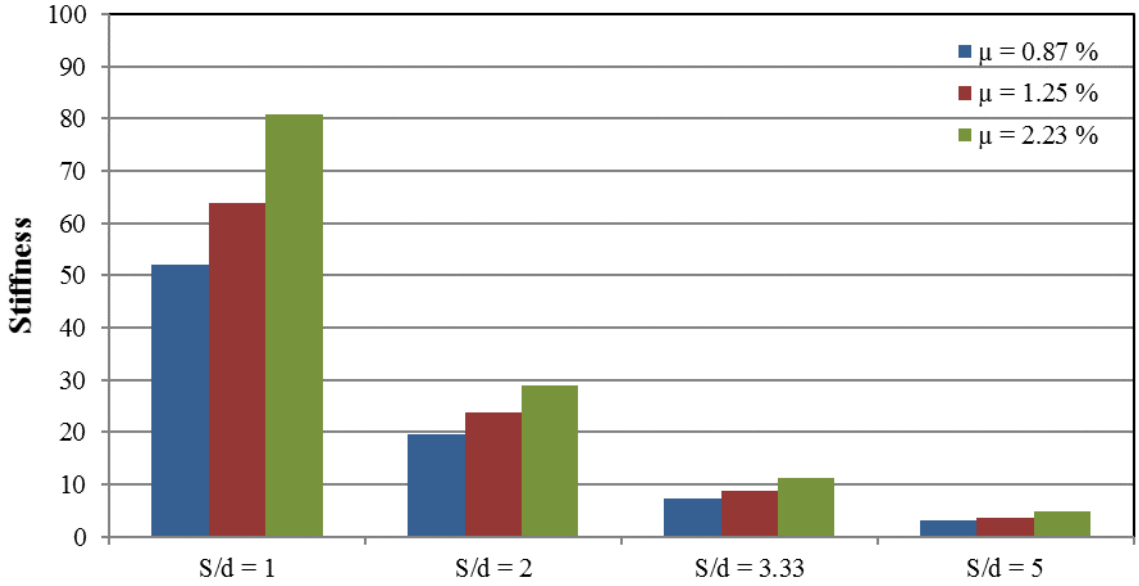

Fig. 15. Effect of S/d and μ on stiffness

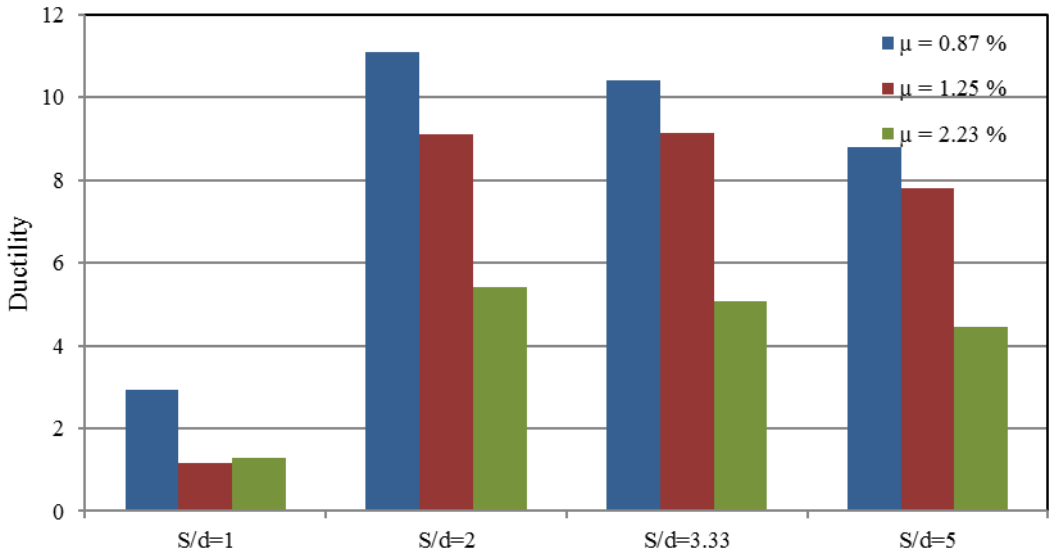

Fig. 16. Effect of μ on ductility

5. CONCLUSIONS

A detailed finite element model is developed in this paper aimed to investigate numerically the behavior of beams made of Engineering Cementitious Composite using PVA fibers and local sand (PVA-ECC). The finite element model is validated against published experimental results. Then, the verified model is utilized in a parametric study to investigate the effect of different parameters, such as shear span-to-depth ratio, shear reinforcement ratio, longitudinal reinforcement ratio and yielding stress of reinforcement, on flexural and shear behavior of PVA-ECC beams. Based on the obtained results, the following conclusions may be drawn:

- PVA-ECC beams have excellent shear capacity even without shear reinforcement. The numerical results indicated that, approximately there is no difference in behavior, failure mode, stiffness, yielding point and peak load point between beams without any shear reinforcement and beams with 6 mm, 8 mm or 10 mm diameter stirrups and 100 mm spacing shear reinforcement. Therefore, shear capacity of ECC is very useful to decrease shear reinforcement congestion especially in structural elements under seismic loads.
- The peak load is increased with increase of longitudinal reinforcement (μ) and with increasing of yielding stress. On the other hand, the peak load is decreased with increase of shear span-to-depth ratio (S/d).
- The mid-span deflection at peak load is increased with the increasing of S/d in all studied cases. The mid-span deflection at peak load is decreased with the increasing values of μ, but beams with μ equal to 1.25 % have higher mid-span deflection than other beams when yielding stress of steel bars is 350 and 420 MPa.
- The stiffness of PVA-ECC is decreased with increasing of S/d and is slightly increased with increasing of μ values also there are minor differences in stiffness when yielding stress of steel reinforcement is changed.
- The beams with S/d equal to 1 have the lower ductility than other S/d ratios. The ductility of beams is decreased with the increasing of longitudinal reinforcement ratio and yielding stress of steel bars.

REFERENCES

[1] H. Fukuyama, Y. Sato, Y. Matsuzaki and H. Mihashi, "Ductile Engineered Cementitious Composite Elements for Seismic Structural Applications," in *12th World Conference on Earthquake Engineering*, Auckland, 2000.

[2] V. C. Li and S. Wang, "Flexural Behaviors of Glass Fiber-Reinforced Polymer (GFRP) Reinforced Engineered Cementitious Composite Beams," *ACI Materials Journal*, vol. 99, no. 1, pp. 11-21, 2002.

[3] A. Hemmati, A. Kheyroddin and M. . K. Sharbatdar, "Flexural Behavior of Reinforced HPFRCC Beams," *Journal of Rehabilitation in Civil Engineering*, pp. 66-77, 2013.

[4] F. Yuan,, J. Pan and C. . K. Leung, "Flexural Behaviors of ECC and Concrete/ECC Composite Beams Reinforced with Basalt Fiber-Reinforced Polymer," *Journal of Composites for Construction (ASCE)*, vol. 17, no. 5, pp. 591-602, 2013.

[5] S. Qudah and M. Maalej, "Application of Engineered Cementitious Composites (ECC) in interior beam–column connections for enhanced seismic resistance," *Engineering Structures*, vol. 69, pp. 235-245, 2014.

[6] A. Alyousif, M. Lachemi, O. Anil, G. Yildirim, M. Sahmaran and A. F. Ashour, "Comparison of shear behaviour of engineered cementitious composite and normal concrete beams with different shear span lengths," *Magazine of Concrete Research*, vol. 68, no. 5, pp. 217-228, 2016.

[7] M. Said, T. S. Mustafa, A. S. Shanour and M. M. Khalil, "Experimental and analytical investigation of high performance concrete beams reinforced with hybrid bars and polyvinyl alcohol fibers," *Construction and Building Materials*, vol. 259, 2020.

[8] D. Meng, T. Huang, Y. . X. Zhang and C. . K. Lee, "Mechanical behaviour of a polyvinyl alcohol fibre reinforced engineered cementitious composite (PVA-ECC) using local ingredients," *Construction and Building Materials*, vol. 141, pp. 259-270, 2017.

[9] J. Feng, W. Sun, L. Chen, B. Chen, E. Arkin, L. Du and M. Pathirage, "Engineered Cementitious Composites using Chinese local ingredients: Material preparation and numerical investigation," *Case Studies in Construction Materials*, vol. 16, 2022.

[10] J. Lubliner, J. Oliver, S. Oller and E. Onate, "A Plastic-Damage Model for Concrte," *Int. J. Solid Structures*, vol. 25, no. 3, pp. 299-326, 1989.

[11] T. Yu, J. G. Teng, Y. L. Wong and S. L. Dong, "Finite Eement Modeling of Confined Concrete-II: Plastic-Damage Model," *Engineering Structures*, pp. 680-691, 2010.

[12] G. G. Triantafyllou, T. C. Rousakis and A. I. Karabinis, "Corroded RC beams patch repaired and strengthened in flexure with fiber-reinforced polymer laminates," *Composites Part B: Engineering*, vol. 112, no. 1, 2017.

[13] U. Cicekli, G. Z. Voyiadjis and R. Abu Al-Rub, "A plasticity and anisotropic damage model for plain concrete," *International Journal of Plasticity*, pp. 1874-1900, 2007.

[14] Dassault Systemes, "Abaqus Analysis User's Guide," Dassault Systèmes Simulia Corp., Rhode Island, 2014.

[15] M. A. Bastian, A. Tambusay, I. Komara, W. Sutrisno, D. Irawan and P. Suprobo, "Enhancing the Ductility of a Reinforced Concrete Beam using Engineered Cementitious Composite," in *Earth and Environmental Science*, Bristol, 2020.

[16] Y. Fang, P. JinLong and W. YuFei, "Numerical study on flexural behaviors of steel reinforced engineered cementitious composite (ECC) and ECC/concrete composite beams," *Science China: Technological Sciences*, vol. 57, no. 3, pp. 637-645, 2014.

[17] D. Meng, C. K. Lee and Y. X. Zhang, "Flexural and shear behaviours of plain and reinforced polyvinyl alcohol-engineered cementitious composite beams," *Engineering Structures*, pp. 261-272, 2017.